CHEMISTRY OF MATERIALS

Article

pubs.acs.org/cm

Extended Conjugation Platinum(II) Porphyrins for use in Near-Infrared Emitting Organic Light Emitting Diodes

Kenneth R. Graham,[†] Yixing Yang,[‡] Jonathan R. Sommer,[†] Abigail H. Shelton,[†] Kirk S. Schanze,*[,†] Jiangeng Xue,*[,‡] and John R. Reynolds*[,†]

[†]Department of Chemistry, Center for Macromolecular Science and Engineering, and [‡]Department of Materials Science and Engineering, University of Florida, Gainesville, Florida 32611-7200, United States

Supporting Information

ABSTRACT: A family of π-extended platinum(II) porphyrins has been synthesized and incorporated into solution processed polymer light emitting diodes (PLEDs) and vapor deposited multilayer organic light emitting diodes (OLEDs), giving rise to devices with peak emission ranging from 771 to 1005 nm. The longest wavelength emitter, platinum(II)-5,10,15,20-(3,5-di-*tert*-butylphenyl)tetraanthroporphyrin (Pt-Ar$_4$TAP), shows an emission maximum at 1005 nm, an external quantum efficiency (EQE) of 0.12%, and a maximum radiant emittance (R_{max}) of 0.23 mW/cm^2 in single layer PLED architectures, which is enhanced to an EQE of 0.20% with an R_{max} of 0.57 mW/cm^2 upon vapor deposition of an electron transport layer. In an effort to understand substituent effects and enhance the performance of π-extended Pt-porphyrins in PLEDs and OLEDs, a family of Pt-tetrabenzoporphyrins (Pt-TBPs) with varying functionality was investigated. The luminescent lifetimes of the Pt-TBPs in solution and in films were measured, and a strong correlation was demonstrated between the film lifetimes and the PLED and OLED efficiencies. An improvement in external quantum efficiency (EQE) from 2.07 to 2.49% for PLEDs and from 8.0 to 9.2% for OLEDs was observed between the less substituted Pt-tetraphenyltetrabenzoporphyrin and the more substituted Pt-5,10,15,20-(3,5-di-*tert*-butylphenyl)tetrabenzoporphyrin. The PLED EQEs were further enhanced to 3.02% with the disubstituted Pt-5,15-(3,5-di-*tert*-butylphenyl)tetrabenzoporphyrin; however, this increase was not observed for the OLEDs where an EQE of 7.8% was measured.

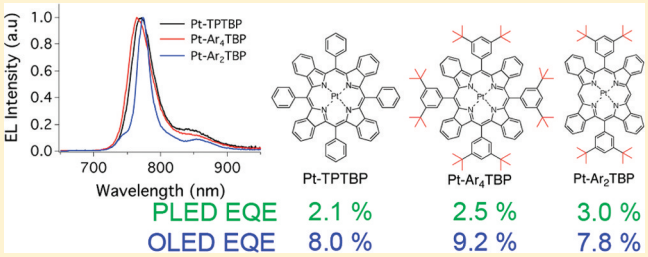

KEYWORDS: *platinum(II) porphyrin, near-infrared, organic light emitting diode, electroluminescence*

INTRODUCTION

Organic light emitting diodes (OLEDs) and polymer light emitting diodes (PLEDs) are of considerable interest owing to their potential for low cost, efficient, flexible, and large area emitting devices.[1] As such, there has been considerable research directed at developing visible light emitting OLEDs and PLEDs, with internal quantum efficiencies reaching nearly 100% and external quantum efficiencies (EQEs) of approximately 20%.[2−5] These high efficiencies have not yet been achieved in the near-infrared (near-IR) region of the electromagnetic spectrum, and currently the most efficient devices have EQEs of ∼8% in the 750−800 nm range and ∼4% in the 850−900 nm range.[6,7] The near-IR region is of considerable interest for applications in infrared signaling, night vision, telecommunications, and wound healing;[8−10] therefore, the further development of near-IR emitting PLEDs and OLEDs is the focus of this work.

The primary strategies for obtaining near-IR emitting PLEDs and OLEDs has been the use of near-IR emitting conjugated polymers,[11−13] lanthanide complexes,[14−19] donor−acceptor based oligomers,[20−23] phosphorescent metal−organic complexes,[24−27] and metalloporphyrins.[6,7,28] The small molecule near-IR emitters are doped into conjugated organic matrices (polymer-PLED or small molecule-OLED) where energy is transferred through charge trapping or Förster processes from the host to the near-IR emitter, thereby resulting in primarily near-IR emission. For the near-IR emitting polymers, the polymer serves as the only material in the active layer. Near-IR emitting conjugated polymers employed in PLEDs show broad emission with wavelength maxima less than 1000 nm with EQEs below 0.5%.[11,12] Lanthanide complexes show narrow emission peaks with emission maxima ranging from 800 to 1600 nm; however, the low photoluminescence quantum yield (ϕ_{em}) of the metal centered F states leads to devices with EQEs below 0.5%.[14−19] Donor−acceptor based fluorescent oligomers feature readily tunable emission from 700 to 1600 nm and have been integrated into OLEDs with device efficiencies in the 1 to 3% range for devices emitting between 700 and 900 nm,[23,29] but dropping below 0.5% for devices emitting in the 1000−1100 nm range.[21] A major shortcoming of the oligomers and other fluorescent materials is that they only emit efficiently from the singlet state, which limits the electroluminescent

Received: August 1, 2011
Revised: November 2, 2011
Published: November 23, 2011

internal quantum efficiencies achievable to approximately 25%. Additionally, near-IR emitting donor–acceptor oligomers with high solution quantum yields (ϕ_{em} > 0.25) have yet to be realized.

Phosphorescent metal–organic complexes are attractive candidates for use in PLEDs and OLEDs, in part because of their high luminescence quantum yields. Additionally, phosphorescent metal–organic complexes have the potential to achieve nearly 100% internal quantum efficiency in device applications because of their ability to efficiently emit from the triplet state as a result of strong spin–orbit coupling.[2,30] Phosphorescent metal–organic complexes with Pt, Ir, or Os as the metal center have been applied to develop devices with relatively high electroluminescence efficiency in the near-IR region with emission occurring primarily in the 700–800 nm range.[24−26] More specifically a subclass of phosphorescent metal–organic complexes, metalloporphyrins, currently show the best performance in near-IR emitting PLEDs or OLEDs, with the most efficient near-IR OLEDs to date based on π-extended Pt-porphyrin complexes such as Pt-tetraphenyltetrabenzoporphyrin (Pt-TPTBP, structures in Figure 1) with a

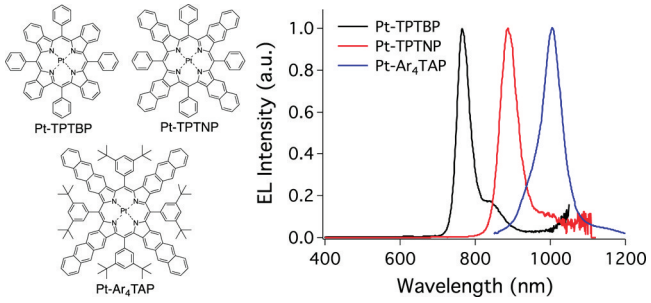

Figure 1. Chemical structures of Pt-TPTBP, Pt-TPTNP, and Pt-Ar_4TAP and the corresponding electroluminescence spectra of the Pt-porphyrin PLEDs consisting of 2% (by weight) of the chromophores in a PVK:PBD (6:4) host.

reported EQE of 8.5% at 765 nm.[6] By further extending the π-system to the Pt-tetraphenyltetranaphthoporphyrin derivative (Pt-TPTNP) the emission wavelength is shifted to 900 nm and, when incorporated into OLEDs, a maximum EQE of 3.8% has been obtained.[7] These Pt-porphyrins show relatively narrow phosphorescence emission bandwidths, and they phosphoresce with the highest emission quantum efficiencies reported to date for emitters in the near-infrared region (λ > 750 nm). Currently, to the best of our knowledge all of the near-IR emitting Pt-porphyrins that have been incorporated into PLEDs or OLEDs have phosphorescence band maxima below 900 nm. Herein, we demonstrate that by further increasing the π-system with a Pt-tetraanthroporphyrin derivative, Pt-Ar_4TAP, the peak electroluminescence wavelength is shifted to ∼1000 nm and Pt-Ar_4TAP is effectively incorporated into PLEDs and multilayer PLEDs with EQEs ranging from 0.1 to 0.2% and peak radiant emittance of 0.57 mW/cm^2. These results are compared directly with devices constructed using Pt-TPTBP and Pt-TPTNP which emit at shorter wavelengths.

The photophysics of various expanded conjugation porphyrins have been previously investigated, and it has been demonstrated that substituents play a major role in determining porphyrin photophysical properties.[31−35] For example, Vinogradov et al. demonstrated that Pd-5,15-diphenyltetrabenzoporphyrin has a phosphorescence quantum yield of 0.15, whereas Pd-5,10,15,20-tetraphenyltetrabenzoporphyrin has a lower quantum yield of only 0.08.[32] This increased quantum yield for the disubstituted derivative originates from the more planar structure, as out-of-plane distorted porphyrins display increased nonradiative decay pathways.[32,34,35] Furthermore, Beeby et al. have demonstrated an approximate doubling of solution ϕ_{em} from 0.11 to 0.21 for 5,10,15,20-tetrasubstituted free base porphyrins when monophenyl substituents are substituted for more bulky fluorene or terphenyl substituents.[33] Drawing from this previous work, a family of Pt-tetrabenzoporphyrins (Pt-TBPs, Figure 2) incorporating 5,15-diaryl and 5,10,15,20-tetraaryl derivatives with varying substituent groups has been synthesized, and the 5,15-diaryl derivatives display a 50% enhancement in solution quantum yield as compared to the 5,10,15,20-tetraaryl derivatives.[36] This family of Pt-TBPs is further characterized through film photoluminescence lifetime measurements, and it is shown that the lifetimes of the various Pt-TBPs are more similar in the solid state as compared to solution, where significant differences in lifetime (and ϕ_{em}) are observed. Additionally, the family of Pt-TBPs is incorporated into PLEDs and OLEDs, and a strong correlation is observed between the film lifetimes and device efficiencies.

RESULTS AND DISCUSSION

Extended Conjugation Platinum(II) Porphyrin Emitters. The series of π-extended tetrabenzo, tetranaphtho, and tetraanthro Pt-porphyrins shown in Figure 1 were synthesized, structurally characterized, and their photophysical properties in solution fully explored as reported in a companion paper.[36] In the present work, we have incorporated these chromophores into near-IR emitting PLEDs and OLEDs. As the π-system is extended across the series Pt-TPTBP, Pt-TPTNP, and Pt-Ar_4TAP the solution emission wavelength maxima shift from 773 to 891 to 1022 nm, respectively, as shown in Table 1. Accompanying this wavelength shift is a decreasing phosphorescence yield (ϕ_{em}) and decreasing lifetime (τ_{em}) as predicted by the energy gap law,[37−39] and discussed in our companion paper.[36] The solution ϕ_{em} value generally provides a good figure of merit to predict the relative efficiencies for a series of structurally related chromophores in a PLED or OLED; therefore, a similar trend of decreasing PLED and OLED efficiency across the series Pt-TPTBP, Pt-TPTNP, and Pt-Ar_4TAP is expected and realized as the emission is shifted further into the near-IR. The emission spectra of the Pt-porphyrin doped PLEDs and OLEDs, shown for the PLEDs in Figure 1, exhibit nearly identical electroluminescence band maxima and band shape as seen for the phosphorescence in solution (Table 1).

PLEDs were fabricated with a sandwich structure consisting of ITO/PEDOT:PSS(40 nm)/emissive layer(110 nm)/LiF(1 nm)/Ca(10 nm)/Al(100 nm), where the emissive layer consists of 2% (by weight) of the Pt-porphyrin in a poly(9-vinylcarbazole) (PVK) and 2-(4-*tert*-butylphenyl)-5-(4-biphenylyl)-1,3,4-oxadiazole (PBD) blend (6:4 by weight) host. This doping concentration results in minimal Pt-porphyrin aggregation and almost no emission from the host matrix. It should be noted that the Pt-Ar_4TAP device does show some visible emission, which is likely due to degradation or impurities since the material is light sensitive and was also difficult to purify. The visible emission is not shown in the spectra because the Pt-Ar_4TAP device was characterized with a near-IR spectrometer; however, the visible emission spectra are included in the Supporting Information, Figure S1. For the radiant emittance

dx.doi.org/10.1021/cm202242x | *Chem. Mater.* 2011, 23, 5305–5312

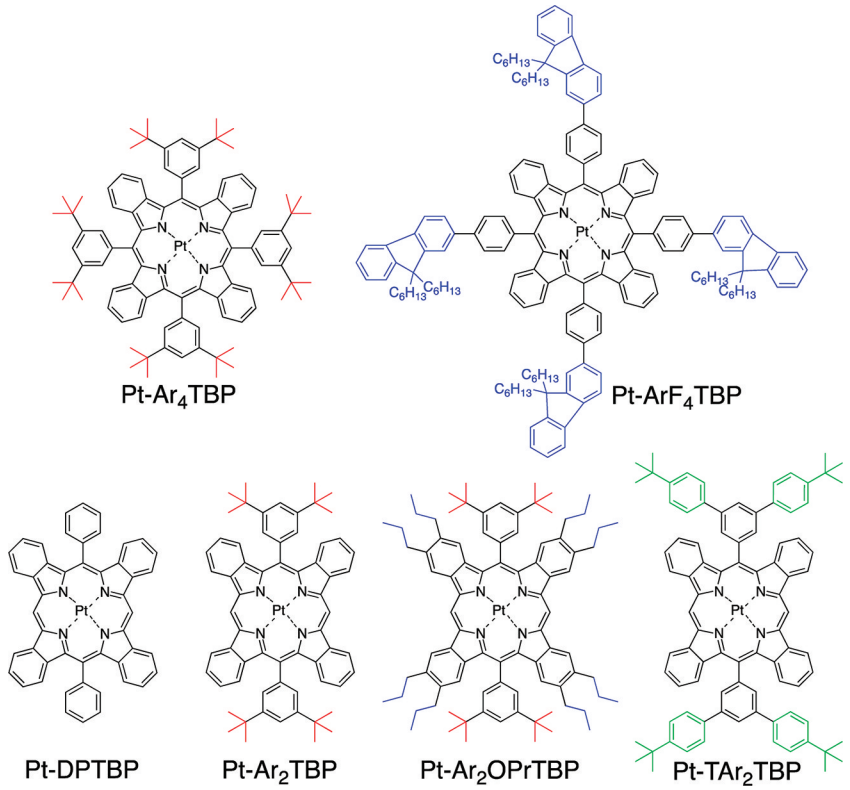

Figure 2. Structures of platinum(II) tetrabenzoporphyrins.

Table 1. Solution Emission Maxima, ϕ_{em}, and Performance Characteristics of Pt-TPTBP, Pt-TPTNP, and Pt- Ar_4TAP Based PLEDs and OLEDs

			λ_{max} EL (nm)		max EQE[d] (%)		R_{max}[d] (mW/cm^2)	
chromophore	λ_{max} PL (nm)- solution[a]	solution ϕ_{em}[a]	PLED[b]	OLED[c]	PLED	OLED	PLED	OLED
Pt-TPTBP	773	0.35	771	773	2.07 ± 0.11	8.0 ± 0.5	1.63 ± 0.02	3.4 ± 0.3
Pt-TPTNP	891	0.15	898	900	0.75 ± 0.05	3.8 ± 0.3	0.67 ± 0.03	1.7 ± 0.2
Pt-Ar_4TAP	1022	0.08	1005	*f*	0.12 ± 0.01	*f*	0.23 ± 0.01	*f*
			1005[e]		0.20 ± 0.03[e]		0.57 ± 0.06[e]	

[a]Solution data is in deoxygenated toluene. [b]PLEDs are with PVK:PBD (6:4) host. [c]OLEDs are with AlQ_3 (Pt-TPTBP), CBP (Pt-TPTNP). [d]All error values are reported as the standard deviation of 4 to 6 different pixels on the same substrate. [e]Values are for multilayer PLEDs with PVK:PBD as host and BPhen as ETL. [f]OLEDs were not fabricated as Pt-Ar_4TAP was unable to be thermally evaporated.

(R) and EQE measurement and calculation, the visible emission from the Pt-Ar_4TAP device was removed by filtering with an 800 nm long-pass filter. The PLEDs show maximum EQEs of 2.07, 0.75, and 0.12%, and maximum near-IR radiant emittance (R_{max}) values of 1.63, 0.67, and 0.23 mW/cm^2 for PLEDs constructed using Pt-TPTBP, Pt-TPTNP, and Pt-Ar_4TAP, respectively, as shown in Table 1. The PLEDs show high turn on voltages between 8 and 17 V with power efficiencies ranging from 0.06 to 2.1 mW/W as listed in Supporting Information, Table S1. The device EQE ratios for Pt-TPTBT to Pt-TPTNP (2.7:1) are in good agreement with the solution ϕ_{em} ratios (2.3:1); however, Pt-Ar_4TAP shows a lower EQE (0.12%) than would be expected from the ϕ_{em} (0.08). The lower than expected EQE for Pt-Ar_4TAP may originate from degradation or impurities as mentioned above. These EQEs and R_{max} values are some of the highest reported for solution processed PLEDs emitting in the 750 − 1050 nm range.

OLEDs were fabricated with a multilayer structure consisting of ITO/NPB(40 nm)/emissive layer/BPhen(80 nm)/LiF(1 nm)/Al(100 nm), where the emissive layer is AlQ_3 with 4 wt % Pt-TPTBP (25 nm) or CBP with 8 wt % Pt-TPTNP (20 nm). Here NPB is N^4,$N^{4\prime}$-di(naphthalen-1-yl)-N^4,$N^{4\prime}$-diphenyl-[1,1′-biphenyl]-4,4′-diamine, BPhen is bathophenanthroline, AlQ_3 is tris-(8-hydroxyquinoline)aluminum, and CBP is 4,4′-bis(*N*-carbazolyl)-1,1′-biphenyl. Pt-Ar_4TAP could not be thermally evaporated because of its high molecular weight; therefore, Pt-Ar_4TAP multilayer PLEDs were constructed by spin-casting a layer of Pt-Ar_4TAP (2% by weight) in PVK:PBD (7:3) onto the PEDOT:PSS coated ITO, followed by thermal evaporation of an electron transporting layer of BPhen (40 nm), and LiF(1 nm)/Al(100 nm)/MoO_x(200 nm). While these device structures may not be fully optimized in terms of layer thickness and doping concentration, they were chosen to provide a common platform to examine the impact of different porphyrin emitters studied here. As the OLEDs were characterized in air without device encapsulation, the purpose of the thermally evaporated MoO_x overlayer, which was only used for the Pt-Ar_4TAP devices, is to improve the OLED device stability as they are exposed to the laboratory ambient for the

dx.doi.org/10.1021/cm202242x | *Chem. Mater.* 2011, 23, 5305–5312

short time period of testing and characterization. The Pt-TPTBP and Pt-TPTNP OLEDs show similar performance as previously reported, with EQE values of 8.0 and 3.8% and R_{max} values of 3.4 and 1.7 mW/cm^2, respectively.[7,28] The addition of the electron transporting layer to the Pt-Ar$_4$TAP device results in an approximate doubling of both the EQE and R_{max} versus the single layer PLED as shown in Table 1. Similar to the PLED performance, the EQE and R_{max} values for Pt-TPTBP and Pt-TPTNP based OLEDs display a similar ratio as the solution quantum yields, whereas the Pt-Ar$_4$TAP devices remain less efficient than the solution quantum yield would suggest.

Effect of Structure on EL Efficiency in Platinum(II) Tetrabenzoporphyrins. The series of platinum(II) tetrabenzophorphyrins in Figure 2 was designed to provide insight as to how structural variation of the expanded conjugation Pt-porphyrins impact their solution and solid state photophysics, and how these properties relate to the PLED and OLED performance. The synthesis, structural and solution photophysical characterization of this series is reported in the companion paper;[36] herein, we characterize the properties of PLEDs and OLEDs that incorporate these chromophores as emitters. The general concept behind the design of this series is based on two different principles; namely, decreasing aggregation and triplet−triplet annihilation processes in the solid state by the addition of bulky and/or solubilizing groups on the chromophores' periphery, and increasing the phosphorescence quantum yield by decreasing the number of aryl groups on the meso positions.[31−33]

The photophysical properties of the Pt-tetrabenzoporphyrins, as listed in Table 2, were studied in solution and doped into films of PVK:PBD (6:4) and polystyrene (PS) at less than 1% by weight. The lifetime of Pt-OEP in polystyrene was also measured to verify agreement with the literature value.[30] The use of PS was compared to PVK:PBD to determine if the film lifetimes were dependent on the polymer matrix, and specifically provide a comparison between an insulating (PS) and a semiconducting matrix (PVK:PBD). As reported in more detail in the companion paper,[36] the solution ϕ_{em} and τ_{em} values are 50−60% larger for the disubstituted 5,15-diaryl porphyrin derivatives relative to the 5,10,15,20-tetraaryl substituted porphyrins. This effect is due to an increased nonradiative decay rate for the tetra-substituted porphyrins, which arises because these complexes have a larger degree of out-of-plane distortion.[32,34,35]

Table 2. Photophysical Data for Pt-Tetrabenzoporphyrins in Degassed Toluene Solutions and Doped into Polystyrene or PVK:PBD Polymer Films at <1% by Weight

porphyrin	ϕ_{em} toluene	τ_{em} / μs toluene	τ_{em} / μs polystyrene	τ_{em} / μs PVK:PBD
Pt-OEP	0.45	(83)[a]	92.7 (91)[b]	c
Pt-TPTBP	0.35	29.9	49.7	45.7
Pt-Ar$_4$TBP	0.33	32.0	51.9	49.8
Pt-ArF$_4$TBP	0.26	20.1	45.6	48.2
Pt-DPTBP	0.30	28.0	c	c
Pt-Ar$_2$TBP	0.49	53.0	64.1	57.5
Pt-TAr$_2$TBP	0.44	51.7	50.5	55.2
Pt-Ar$_2$OPrTBP	0.45	51.8	52.1	52.0

[a]Value taken from Thompson, et al.[40] [b]Value in parentheses taken from Forrest et al.[30] [c]Values not determined.

On the basis of this solution behavior, at the outset we predicted that the disubstituted porphyrins would give rise to more efficient PLEDs and OLEDs. However, photophysical data on the chromophores in the solid state is likely a better predictor for device performance. As seen in Table 2, the lifetimes of the Pt-tetrabenzoporphyrins in polystyrene are relatively close (within 12%) to those in PVK:PBD, indicating that the lifetimes are not overly sensitive to the nature of the polymer matrix. Since PVK:PBD is the host matrix used in the PLEDs, we will focus the discussion on this set of lifetime data. The most striking feature of the solid state emission lifetime data is that the 5,10,15,20-tetraaryl substituted Pt-porphyrins exhibit substantially longer τ_{em} (ranging from 50−140% increase) in the PVK:PBD matrix compared to that observed for the same complexes in solution. By contrast, the 5,15-diaryl substituted Pt-porphyrins exhibit small or negligible difference in τ_{em} for the complexes dispersed in polymer films compared to solutions. The increased lifetimes in film compared to solution are attributed to suppression of nonradiative decay pathways by the rigid polymer matrix. This effect is more pronounced for the saddle shaped tetra-substituted derivatives than for the planar disubstituted derivatives.[28,32,41] For example, in solution τ_{em} of Pt-Ar$_2$TBP is 66% larger than that of Pt-Ar$_4$TBP, while the lifetime of Pt-Ar$_2$TBP in PVK:PBD is only 15% longer than that of Pt-Ar$_4$TBP in PVK:PBD. The effect of the polymer matrix on the lifetime of the Pt-porphyrins is similar to the effect seen for chromophores in low temperature solvent glasses, where nonradiative decay pathways arising from large motion vibrational, torsional, and librational modes are suppressed.[41] Since nonradiative decay pathways are more dominant for the tetra-substituted porphyrins, the rigid polymer matrix has a significantly larger effect on these chromophores.[41]

There are several important conclusions that can be drawn from this comparison of the Pt-tetrabenzoporphyrin emission lifetime data in solution and films. First, it is evident that the trends observed when comparing the τ_{em} and ϕ_{em} values for the series of benzoporphyrins in solution *do not* directly carry over

Table 3. PLED and OLED Critical Parameters for Pt-TBP Derivatives in PVK:PBD (PLEDs) and in AlQ$_3$ (OLEDs)

	λ_{max} EL (nm)		max EQE (%)		R_{max} (mW/cm^2)	
chromophore	PLED	OLED	PLED	OLED	PLED	OLED
Pt-TPTBP	771	773	2.07 ± 0.11	8.0 ± 0.5	1.63 ± 0.02	3.4 ± 0.3
Pt-Ar$_4$TBP	764	773	2.49 ± 0.16	9.2 ± 0.6	1.93 ± 0.07	4.4 ± 0.3
Pt-ArF$_4$TBP	774	NA	2.56 ± 0.18	NA	2.19 ± 0.03	NA
Pt-DPTBP	NA	777	NA	5.0 ± 0.3	NA	2.1 ± 0.2
Pt-Ar$_2$TBP	774	777	3.02 ± 0.10	7.8 ± 0.5	2.23 ± 0.08	3.0 ± 0.3
Pt-TAr$_2$TBP	775	777	2.49 ± 0.11	3.2 ± 0.3	1.88 ± 0.05	1.9 ± 0.2
Pt-Ar$_2$OPrTBP	790	792	2.70 ± 0.19	6.8 ± 0.4	2.20 ± 0.09	3.2 ± 0.3

dx.doi.org/10.1021/cm202242x | Chem. Mater. 2011, 23, 5305−5312

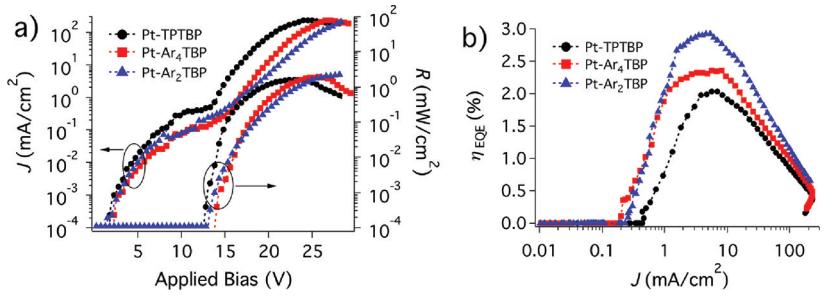

Figure 3. PLED current density–voltage-radiant emittance (*J-V-R*) plot (a) and EQE plot (b) for Pt-TPTBP, Pt-Ar_4TBP, and Pt-Ar_2TBP in PVK:PBD.

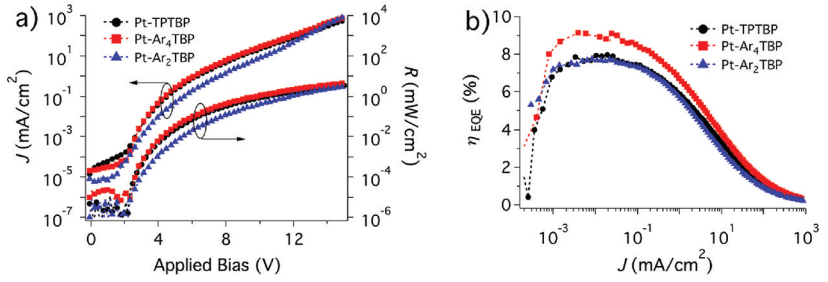

Figure 4. OLED *J-V-R* plot (a) and EQE plot (b) for PtTPTBP, $PtAr_4$TBP, and $PtAr_2$TBP.

to the solid state. The results indicate that the lifetimes for the series of di- and tetra-substituted Pt-benzoporphyrins are more similar in the solid films compared to in solution. Although the solid state ϕ_{em} values were not determined, given that excited state decay of these Pt-porphyrins is dominated by nonradiative decay channels,[36] we anticipate that the trends in ϕ_{em} for the series in the polymers run parallel to τ_{em}. Thus, while the solution photophysical data gives rise to the prediction that the disubstituted porphyrins will give more efficient electroluminescence in the devices, the film results contradict this, suggesting that in the absence of other factors, the entire set of porphyrins should exhibit more comparable device efficiencies.

PLEDs based on the Pt-tetrabenzoporphyrin family with the chromophores doped into PVK:PBD at 2% by weight were fabricated and characterized in the same device structure employed for the series of expanded conjugation porphyrins. The PLED data is compared between devices made at the same time using identical processing methods and conditions to eliminate set-to-set variation. In addition, multiple sets of devices were fabricated and evaluated, and all displayed the same general trends. The PLED critical parameters are shown in Table 3, and plots of the current, voltage, and near-IR radiant emittance along with the EQE-current flux relationships are shown in Figure 3. It is evident from Figure 3 that the PLEDs exhibit significant current leakage before the devices begin to turn on. All of the Pt-tetrabenzorphyrin derivatives show turn-on voltages between 12.3 and 15.6 V, as listed in Supporting Information, Table S2, with maximum EQEs occurring at *R* values between 0.18 and 0.23 mW/cm^2 in the PLEDs. The high turn-on and operating voltages are due to the thickness of the PVK:PBD layer (110 nm) and the large barriers to charge injection. These high turn-on voltages may be reduced by employing electron and/or hole injection layers or reducing the PVK:PBD layer thickness.[3,7,42,43]

The Pt-tetrabenzoporphyrin PLED data shown in Table 3 and Figure 3 displays two notable trends, namely, an increase in EQE upon introduction of bulky substituents, and a higher EQE for the disubstituted Pt-Ar_2TBP compared the tetra-substituted Pt-Ar_4TBP. Beginning with the 5,10,15,20-tetrasubstituted derivatives, an increase in EQE from 2.07 ± 0.11 to 2.49 ± 0.16% and an increase in R_{max} from 1.63 ± 0.02 to 1.93 ± 0.07 mW/cm^2 is observed when the phenyl substituents in Pt-TPTBP are replaced with the more bulky 3,5-di-*tert*-butylphenyl substituents in Pt-Ar_4TBP as shown in Figure 3. This increase in efficiency and *R* is in accordance with that previously reported by others, and likely originates from decreased aggregation and decreased triplet–triplet annihilation processes afforded by the bulkier 3,5-di-*tert*-butylphenyl substituents.[31] No significant difference is observed between the 3,5-di-*tert*-butylphenyl (Pt-Ar_4TBP) and the fluorene (Pt-ArF_4TBP) derivatives, suggesting that the 3,5-di-*tert*-butylphenyl group is sufficiently bulky to suppress aggregation or dimerization in the films. In comparing the 5,15-diaryl and 5,10,15,20-tetraaryl derivatives, a 20% increase in EQE from 2.49 ± 0.16 to 3.02 ± 0.10% is observed for the disubstituted Pt-Ar_2TBP derivative compared to the tetra-substituted Pt-Ar_4TBP derivative. This increase is less than the 48% increase the solution quantum yield would predict (0.49 vs 0.33), but this is expected given the difference in the τ_{em} values in the PVK:PBD films (49.8 vs 57.5 μs). The other disubstituted derivatives, Pt-TAr_2TBP and Pt-Ar_2OPrTBP, did not show a statistically significant difference in EQE as compared to the tetrasubstituted derivatives. These PLED results, along with the film emission data, indicate that increases in solution quantum efficiency for this family of Pt-tetrabenzoporphyrins does not directly translate to increased device efficiencies. Alternatively, the film emission lifetimes show a good correlation with PLED efficiencies. For example, the complexes with the shortest and longest emission lifetimes in PVK:PBD are Pt-TPTBP and Pt-Ar_2TBP, respectively (45.7 and 57.5 μs); in correlation with the Pt-TPTBP devices giving the lowest EQE at 2.07 ± 0.11%, while those that incorporate Pt-Ar_2TBP give the highest at 3.02 ± 0.10. The bathochromic shift of the emission maximum observed for the octapropyl substituted Pt-Ar_2OPrTBP

dx.doi.org/10.1021/cm202242x | *Chem. Mater.* 2011, 23, 5305–5312

derivative to 790 nm is attributed to the addition of the 8 weakly electron donating propyl substitutents.

We also fabricated and tested OLEDs featuring a multilayer structure of ITO/NPB(40 nm)/AlQ_3:4 wt %Pt porphyrin(25 nm)/BPhen(80 nm)/LiF(1 nm)/Al(100 nm). The OLEDs show lower turn-on voltages (Supporting Information, Table S2), lower leakage currents, higher efficiencies, and higher R values than the PLEDs as evident in comparing Figures 3 and 4 and the data presented in Table 3. This is attributed to the multilayer structure that facilitates charge injection and serves to maintain charge balance and confine the recombination zone to the emissive layer;[2,4,44,45] additionally, the vapor deposited materials may be of higher purity because of enhancement from the thermal evaporation process.

For the OLEDs, a maximum EQE of 9.2% and R_{max} of 4.4 mW/cm^2 is achieved with Pt-Ar_4TBP. This is higher than the corresponding tetraphenyl derivative, Pt-TPTBP, and may be attributed to suppression of triplet−triplet annihilation because of decreased porphyrin/porphyrin interactions resulting from the more bulky 3,5-di-*tert*-butylphenyl groups. Similarly, the diphenyl derivative, Pt-DPTBP, shows significantly lower EQE and R_{max} than Pt-Ar_2TBP. In contrast to the PLED results and what the lifetimes in PVK:PBD suggest, Pt-Ar_2TBP exhibits a lower EQE and R_{max} than Pt-Ar_4TBP in the OLEDs. This differing trend may be due to the different interactions of the Pt-tetrabenzoporphyrins with the AlQ_3 matrix versus the PVK:PBD matrix. The electroluminescent (EL) lifetimes, which Forrest et al. have previously shown to be comparable to the photoluminescent (PL) lifetimes,[30] of Pt-Ar_4TBP and Pt-Ar_2TBP were measured to be 27.0 and 26.5 μs, respectively, in the OLEDs operated at a current density of J = 10 mA/cm^2 (with AlQ_3 host). These lifetimes are significantly shorter than the photoluminescent lifetimes in PVK:PBD (49.8 and 57.5 μs for Pt-Ar_4TBP and Pt-Ar_2TBP, respectively); note also that Pt-Ar_2TBP does not display a longer lifetime than Pt-Ar_4TBP as was observed in the PL lifetimes in the PVK:PBD host. Similar decreased emission lifetimes in AlQ_3 compared to polystyrene were previously reported by Thompson and co-workers for Pt-OEP and two other complexes.[30,40]

The bulkier disubstituted derivatives, Pt-TAr_2TBP and Pt-Ar_2OPrTBP, were also tested in OLEDs and compared with the Pt-Ar_2TBP derivative. Both of these derivatives show lower EQEs and R_{max} values than for Pt-Ar_2TBP. Correspondingly, the Pt-TAr_2TBP and Pt-Ar_2OPrTBP based OLEDs also possess shorter EL lifetimes, 19.2 and 23.6 μs, respectively (also at J = 10 mA/cm^2), than the Pt-Ar_2TBP device. This suggests that the Pt-Ar_2TBP is already well-dispersed in the film with minimal porphyrin-porphyrin interactions. The reason for the significant decrease in EQE from Pt-Ar_2TBP to Pt-TAr_2TBP is not known; however, since this decrease is not evident for the PLEDs it may arise from the differing interactions of the porphyrin with the host matrix. As was observed for the PLEDs, the trend in the OLED film lifetimes (26.5, 23.6, and 19.2 μs) correspond with the EQEs (7.8, 6.8, 3.2%) for Pt-Ar_2TBP, Pt-Ar_2OPrTBP, and Pt-TAr_2TBP based OLEDs, respectively.

SUMMARY AND CONCLUSIONS

In conclusion we have demonstrated the incorporation of a family of π-extended Pt-porphyrins, including the novel Pt-Ar_4TAP derivative, into PLEDs and OLEDs. Through the extension of the π-system to Pt-Ar_4TAP the electroluminescence was shifted to 1005 nm, which is the longest wavelength demonstrated to date for a triplet phosphor in an electroluminescent device. The photophysics, PLED, and OLED data on this series of π-extended Pt-porphyrins were compared, revealing decreasing solution ϕ_{em} and device efficiency as the π-system is extended and the emission is bathochromically shifted from ∼770 nm to ∼1005 nm. The photophysics of a series of variously substituted Pt-tetrabenzoporphyrins were characterized both in solution and in film and compared with their performance in PLEDs and OLEDs. Although relatively large differences in ϕ_{em} and τ_{em} were observed in solution, the difference in τ_{em} was considerably less in polystyrene and PVK:PBD polymer film matrices. The results of this study clearly demonstrate that the large differences observed for the solution ϕ_{em} do not directly correlate with the performance of the chromophores in devices; on the other hand, the solid state τ_{em} is demonstrated as an accurate predictor of relative device performance both in PLEDs and in OLEDs. It was also found that the addition of 3,5-di-*tert*-butylphenyl groups in place of phenyl groups on the benzoporphyrin ring periphery results in increased device efficiency; however, further increasing the size of the substitutents to fluorene or terphenyl groups does not improve the device performance. Although the efficiency improvements obtained with the disubstituted Pt-benzoporphyrins were not as high as predicted by their solution ϕ_{em} values, record high EQEs were obtained for PLEDs and OLEDs emitting in the near-IR with EQEs of 3.0 and 9.2%, respectively, for Pt-Ar_2TBP (PLED) and Pt-Ar_4TBP (OLED).

EXPERIMENTAL SECTION

Materials. The Pt-porphyrins were synthesized and purified as reported in the companion paper.[36] All other materials were purchased and used as received, with the exception of chlorobenzene which was purchased anhydrous and was deoxygenated by freeze−pump−thawing.

Optical Characterization. The methods used to obtain the solution photophysical data are described in the companion paper.[36] Solution lifetimes were determined from transient absorbance measurements while film lifetimes were determined by photoluminescence decay. Films of the Pt-TBPs in polystyrene (PS) or PVK:PBD were prepared by spin coating the Pt-TBP:PS or Pt-TBP:PVK:PBD (Pt-TBP was less than 1% by weight relative to PVK:PBD or PS) in anhydrous and deoxygenated chlorobenzene solutions onto PEDOT:PSS coated glass slides in an argon atmosphere glovebox (<0.1 ppm O_2 and H_2O). The films were stored in the glovebox for at least one week prior to measuring the film lifetimes. The films were removed individually from the glovebox in a sealed custom-built borosilicate glass chamber to eliminate exposure to oxygen. Phosphorescence lifetimes of the porphyrin-doped films were obtained with an in-house built instrument that used a Spex 0.25 m double monochromator for wavelength selection, a Hamamatsu R928 photomultiplier tube for optical detection, and a Tektronix TDS-3032B digital oscilloscope for data acquisition. A Coherent Cube diode laser operating at 405 nm in pulsed mode was used as the excitation source.

PLED Fabrication and Characterizaiton. Prepatterned ITO on glass substrates (15 Ω/□, 25 × 25 mm) were cleaned through sequentially sonicating in a sodium dodecyl sulfate solution, deionized (18 MΩ) water, acetone, and isopropanol for 15 min each. Substrates were then oxygen plasma cleaned for 20 min, a film of PEDOT:PSS (Clevios P VP Al 4083) was deposited by spin-casting at 4000 rpm, and annealed on a hot plate in an argon glovebox for 20 min at 130 °C. Individual solutions of PVK (20 mg/mL), PBD (20 mg/mL), Pt-porphyrin (3.5 mg/mL) were prepared in anhydrous and deoxygenated chlorobenzene and stirred overnight. Solutions were combined to give 6:4 (by weight) PVK:PBD ratio, or 7:3 for Pt-Ar_4TAP multilayer PLED, with 2% (by weight) Pt-porphyrin. The resulting solution mixtures were filtered with 0.45 μm PTFE (Whatman puradisc) filters and using a clean glass syringe they were

directly deposited onto the PEDOT:PSS coated ITO. The solutions were spin-cast at 1000 rpm for 60 s, and with the exception of the multilayer Pt-Ar_4TAP PLED, followed by thermal evaporation of LiF (1 nm), Ca (10 nm), and Al (100 nm) at a pressure of 1×10^{-6} mbar through shadow masks. Following spin-casting of the active layer in the multilayer Pt-Ar_4TAP PLED, the device was taken to the Xue laboratory utilizing a covered and sealed glass chamber under vacuum to minimize air and light exposure. A layer of BPhen was then thermally evaporated followed by LiF, Al, and MoO_x at the thicknesses reported in the text. The PEDOT:PSS layer was ~40 nm thick, and the active layer was ~110 nm thick as determined by AFM for all devices. Each ITO substrate consisted of 8 independently addressable pixels of area 7.07 mm^2. Eight devices could be processed simultaneously, and to minimize set-to-set variations all Pt-TBP results are presented for devices made in the same device set with averages of 5 to 7 pixels reported along with the standard deviations. All device testing was performed in ambient atmosphere immediately after the device was removed from the glovebox. PLED spectra were measured with an ISA Spex Triax 180 spectrograph coupled to a Spectrum-1 liquid nitrogen cooled silicon CCD detector for the Pt-TBPs and Pt-TPTNP, or a Spex Fluorolog II equipped with an InGaAs near-IR photomultiplier tube detector for Pt-Ar_4TAP with the devices kept at a constant current by a Keithley 2400 sourcemeter. *J-V-R* measurements were performed with LabVIEW being used to scan the applied bias of the Keithley 2400 sourcemeter while measuring the optical power output with a calibrated UDT silicon photodiode coupled with a UDT optometer. Radiant emittance values were calculated assuming Lambertian emission, and EQE values were calculated following the recommended methods for both the PLEDs and the OLEDs.[46]

OLED Fabrication and Characterization. OLEDs were fabricated on prepatterned ITO/glass substrates which were cleaned through sequential sonication in deionized water, acetone, and isopropanol for 15 min each followed by exposure to an ultraviolet ozone environment for 15 min immediately prior to loading into a high vacuum thermal evaporator. All layers were deposited by thermal evaporation at a base pressure of 1×10^{-7} Torr following previously published procedures.[44] Each Indium Tin Oxide (ITO)/glass substrate featured four OLED pixels of 4 mm^2 active device area with the electrodes in a cross-bar geometry. *J-V-R* measurements were performed in ambient atmosphere using an Agilent 4155C semiconductor parameter analyzer and a calibrated Newport silicon photodiode. Electroluminescence spectra of the Pt-TBPs were collected with an OceanOptics HR400, and spectra for Pt-TPTNP were collected with an ISA Spex Triax 180 spectrograph coupled to a Spectrum-1 liquid nitrogen silicon CCD detector, with devices driven at a constant current using a Keithley 2400 source meter. All measurements presented are averages over 10 pixels and are presented along with standard deviations. Electroluminescence transient lifetimes were measured by applying 1 ms voltage pulses to the devices and measuring the decay of the electroluminescence. The voltages were created by a Tektronix AFG3101 function generator (100 MHz), and the magnitude of voltages was chosen to keep the current density at 10 mA/cm^2. The decay signals were captured by a Newport 818-UV photodetector, which was connected with a Tektronix DPO3054 digital phosphor oscilloscope (500 MHz) for data acquisition.

■ ASSOCIATED CONTENT

Supporting Information

The visible emission spectra for the Pt-Ar_4TAP based PLED and OLED, turn on voltages, and power efficiencies for all Pt-porphyrin PLEDs and OLEDs. This material is available free of charge via the Internet at http://pubs.acs.org.

■ AUTHOR INFORMATION

Corresponding Author

*E-mail: reynolds@chem.ufl.edu (J.R.R.), jxue@mse.ufl.edu (J.X.), kschanze@chem.ufl.edu (K.S.S.).

■ ACKNOWLEDGMENTS

We gratefully acknowledge financial support from the U.S. Army Aviation and Missile Research, Development, and Engineering Center (AMRDEC) (Project No. W31P4Q-08-1-0003).

■ REFERENCES

(1) D'andrade, B. W.; Forrest, S. R. *Adv. Mater.* **2004**, *16*, 1585–1595.
(2) Adachi, C.; Baldo, M. A.; Thompson, M. E.; Forrest, S. R. *J. Appl. Phys.* **2001**, *90*, 5048–5051.
(3) Yang, X. H.; Muller, D. C.; Neher, D.; Meerholz, K. *Adv. Mater.* **2006**, *18*, 948–954.
(4) Eom, S.-H.; Zheng, Y.; Wrzesniewski, E.; Lee, J.; Chopra, N.; So, F.; Xue, J. *Org. Electron.* **2009**, *10*, 686–691.
(5) Eom, S.-H.; Zheng, Y.; Wrzesniewski, E.; Lee, J.; Chopra, N.; So, F.; Xue, J. *Appl. Phys. Lett.* **2009**, *94*, 153303.
(6) Sun, Y.; Borek, C.; Hanson, K.; Djurovich, P. I.; Thompson, M. E.; Brooks, J.; Brown, J. J.; Forrest, S. R. *Appl. Phys. Lett.* **2007**, *90*, 213503.
(7) Sommer, J. R.; Farley, R. T.; Graham, K. R.; Yang, Y. X.; Reynolds, J. R.; Xue, J. G.; Schanze, K. S. *ACS Appl. Mater. Interfaces* **2009**, *1*, 274–278.
(8) Ratches, J. A. *Ferroelectrics* **2006**, *342*, 183–192.
(9) Suzuki, H. *J. Photochem. Photobiol., A* **2004**, *166*, 155–161.
(10) Whelan, H. T.; Smits, R. L.; Buchman, E. V.; Whelan, N. T.; Turner, S. G.; Margolis, D. A.; Cevenini, V.; Stinson, H.; Ignatius, R.; Martin, T.; Cwiklinski, J.; Philippi, A. F.; Graf, W. R.; Hodgson, B.; Gould, L.; Kane, M.; Chen, G.; Caviness, J. *J. Clin. Laser Med. Surg.* **2001**, *19*, 305–314.
(11) Thompson, B. C.; Madrigal, L. G.; Pinto, M. R.; Kang, T.-S.; Schanze, K. S.; Reynolds, J. R. *J. Polym. Sci., Part A: Polym. Chem.* **2005**, *43*, 1417–1431.
(12) Yang, R. Q.; Tian, R. Y.; Yan, J. G.; Zhang, Y.; Yang, J.; Hou, Q.; Yang, W.; Zhang, C.; Cao, Y. *Macromolecules* **2005**, *38*, 244–253.
(13) Baigent, D. R.; Hamer, P. J.; Friend, R. H.; Moratti, S. C.; Holmes, A. B. *Synth. Met.* **1995**, *71*, 2175–2176.
(14) Sun, R. G.; Wang, Y. Z.; Zheng, Q. B.; Zhang, H. J.; Epstein, A. J. *J. Appl. Phys.* **2000**, *87*, 7589–7591.
(15) Harrison, B. S.; Foley, T. J.; Bouguettaya, M.; Boncella, J. M.; Reynolds, J. R.; Schanze, K. S.; Shim, J.; Holloway, P. H.; Padmanaban, G.; Ramakrishnan, S. *Appl. Phys. Lett.* **2001**, *79*, 3770–3772.
(16) Harrison, B. S.; Foley, T. J.; Knefely, A. S.; Mwaura, J. K.; Cunningham, G. B.; Kang, T. S.; Bouguettaya, M.; Boncella, J. M.; Reynolds, J. R.; Schanze, K. S. *Chem. Mater.* **2004**, *16*, 2938–2947.
(17) Kawamura, Y.; Wada, Y.; Yanagida, S. *Jpn. J. Appl. Phys., Part 1* **2001**, *40*, 350–356.
(18) de Bettencourt-Dias, A. *Dalton Trans.* **2007**, 2229–2241.
(19) Katkova, M. A.; Bochkarev, M. N. *Dalton Trans.* **2010**, *39*, 6599–6612.
(20) Qian, G.; Dai, B.; Luo, M.; Yu, D. B.; Zhan, J.; Zhang, Z. Q.; Ma, D. G.; Wang, Z. Y. *Chem. Mater.* **2008**, *20*, 6208–6216.
(21) Qian, G.; Zhong, Z.; Luo, M.; Yu, D. B.; Zhang, Z. Q.; Wang, Z. Y.; Ma, D. G. *Adv. Mater.* **2009**, *21*, 111–116.
(22) Yang, Y.; Farley, R. T.; Steckler, T. T.; Eom, S.-H.; Reynolds, J. R.; Schanze, K. S.; Xue, J. *Appl. Phys. Lett.* **2008**, *93*, 163305.
(23) Yang, Y.; Farley, R. T.; Steckler, T. T.; Eom, S.-H.; Reynolds, J. R.; Schanze, K. S.; Xue, J. *J. Appl. Phys.* **2009**, *106*, 044509.
(24) Williams, E. L.; Li, J.; Jabbour, G. E. *Appl. Phys. Lett.* **2006**, *89*, 083506.
(25) Cocchi, M.; Kalinowski, J.; Virgili, D.; Williams, J. A. G. *Appl. Phys. Lett.* **2008**, *92*, 113302.
(26) Lee, T. C.; Hung, J. Y.; Chi, Y.; Cheng, Y. M.; Lee, G. H.; Chou, P. T.; Chen, C. C.; Chang, C. H.; Wu, C. C. *Adv. Funct. Mater.* **2009**, *19*, 2639–2647.
(27) Yan, F.; Li, W. L.; Chu, B.; Liu, H. H.; Zhang, G.; Su, Z. S.; Zhu, J. Z.; Han, L. L.; Li, T. L.; Chen, Y. R.; Cheng, C. H.; Fan, Z. Q.; Du, G. T. *Org. Electron.* **2009**, *10*, 1408–1411.

(28) Borek, C.; Hanson, K.; Djurovich, P. I.; Thompson, M. E.; Aznavour, K.; Bau, R.; Sun, Y. R.; Forrest, S. R.; Brooks, J.; Michalski, L.; Brown, J. *Angew. Chem., Int. Ed.* **2007**, *46*, 1109−1112.
(29) Qian, G.; Zhong, Z.; Luo, M.; Yu, D.; Zhang, Z.; Ma, D.; Wang, Z. Y. *J. Phys. Chem. C* **2009**, *113*, 1589−1595.
(30) Baldo, M. A.; O'Brien, D. F.; You, Y.; Shoustikov, A.; Sibley, S.; Thompson, M. E.; Forrest, S. R. *Nature* **1998**, *395*, 151−154.
(31) Ikai, M.; Ishikawa, F.; Aratani, N.; Osuka, A.; Kawabata, S.; Kajioka, T.; Takeuchi, H.; Fujikawa, H.; Taga, Y. *Adv. Funct. Mater.* **2006**, *16*, 515−519.
(32) Lebedev, A. Y.; Filatov, M. A.; Cheprakov, A. V.; Vinogradov, S. A. *J. Phys. Chem. A* **2008**, *112*, 7723−7733.
(33) Barker, C. A.; Zeng, X. S.; Bettington, S.; Batsanov, A. S.; Bryce, M. R.; Beeby, A. *Chem.—Eur. J.* **2007**, *13*, 6710−6717.
(34) Knyukshto, V. N.; Sagun, E. I.; Shul'ga, A. M.; Bachilo, S. M.; Starukhin, D. A.; Zen'kevich, E. I. *Opt. Spectrosc.* **2001**, *90*, 67−77.
(35) Roder, B.; Buchner, M.; Ruckmann, I.; Senge, M. O. *Photochem. Photobiol. Sci.* **2010**, *9*, 1152−1158.
(36) Sommer, J. R.; Shelton, A. H.; Parthasarathy, A.; Ghiviriga, I.; Reynolds, J. R.; Schanze, K. S. *Chem. Mater.* **2011**, in press, DOI: 10.1021/cm202241e.
(37) Siebrand, W. *J. Chem. Phys.* **1966**, *44*, 4055−4057.
(38) Caspar, J. V.; Kober, E. M.; Sullivan, B. P.; Meyer, T. J. *J. Am. Chem. Soc.* **1982**, *104*, 630−632.
(39) Siebrand, W. *J. Chem. Phys.* **1967**, *46*, 440−447.
(40) Kwong, R. C.; Sibley, S.; Dubovoy, T.; Baldo, M.; Forrest, S. R.; Thompson, M. E. *Chem. Mater.* **1999**, *11*, 3709−3713.
(41) Gentemann, S.; Nelson, N. Y.; Jaquinod, L.; Nurco, D. J.; Leung, S. H.; Medforth, C. J.; Smith, K. M.; Fajer, J.; Holten, D. *J. Phys. Chem. B* **1997**, *101*, 1247−1254.
(42) Cheng, Y.-J.; Liu, M. S.; Zhang, Y.; Niu, Y.; Huang, F.; Ka, J.-W.; Yip, H.-L.; Tian, Y.; Jen, A. K. Y. *Chem. Mater.* **2007**, *20*, 413−422.
(43) Huang, F.; Shih, P. I.; Liu, M. S.; Shu, C. F.; Jen, A. K. Y. *Appl. Phys. Lett.* **2008**, *93*, 243302.
(44) Zheng, Y.; Eom, S.-H.; Chopra, N.; Lee, J.; So, F.; Xue, J. *Appl. Phys. Lett.* **2008**, *92*, 223301.
(45) Chopra, N.; Lee, J.; Zheng, Y.; Eom, S.-H.; Xue, J.; So, F. *ACS Appl. Mater. Interfaces* **2009**, *1*, 1169−1172.
(46) Forrest, S. R.; Bradley, D. D. C.; Thompson, M. E. *Adv. Mater.* **2003**, *15*, 1043−1048.